JACS
JOURNAL OF THE AMERICAN CHEMICAL SOCIETY

Article

pubs.acs.org/JACS

Intermolecular Headgroup Interaction and Hydration as Driving Forces for Lipid Transmembrane Asymmetry

Nikolay Smolentsev,[‡] Cornelis Lütgebaucks,[‡] Halil I. Okur, Alex G. F. de Beer, and Sylvie Roke*

Laboratory for Fundamental BioPhotonics (LBP), Institute of Bioengineering (IBI), and Institute of Materials Science (IMX), School of Engineering (STI), and Lausanne Centre for Ultrafast Science (LACUS), École Polytechnique Fédérale de Lausanne (EPFL), CH-1015 Lausanne, Switzerland

Supporting Information

ABSTRACT: Variations between the inner and outer leaflets of cell membranes are crucial for cell functioning and signaling, drug−membrane interactions, and the formation of lipid domains. Transmembrane asymmetry can in principle be comprised of an asymmetric charge distribution, differences in hydration, specific headgroup/H-bonding interactions, or a difference in the number of lipids per leaflet. Here, we characterize the transmembrane asymmetry of small unilamellar liposomes consisting of zwitterionic and charged lipids in aqueous solution using vibrational sum frequency scattering and second harmonic scattering, label-free methods, specifically sensitive to lipid and water asymmetries. For single component liposomes, transmembrane asymmetry is present for the charge distribution and lipid hydration, but the leaflets are not detectably asymmetric in terms of the number of lipids per leaflet, even though geometrical packing arguments would predict so. Such a lipid transmembrane asymmetry can, however, be induced in binary lipid mixtures under conditions that enable H-bonding interactions between phosphate and amine groups. In this case, the measured asymmetry consists of a different number of lipids in the outer and inner leaflet, a difference in transmembrane headgroup hydration, and a different headgroup orientation for the interacting phosphate groups.

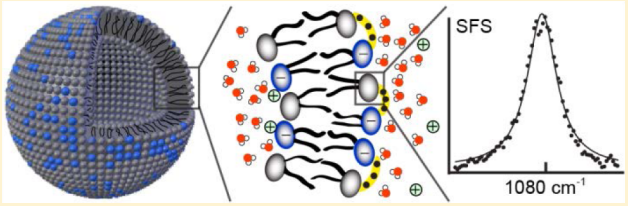

INTRODUCTION

Compositional diversity between the inner and outer leaflets of cellular and organelle membranes are crucial for cell functioning. Nonrandom and nonequal leaflet composition occurs in eukaryotic membranes.[1−3] Certain lipids, such as glycolipids, phosphatidylcholine (PC), and sphingomyelin, are predominantly present in the outer leaflet, whereas others, such as phosphatidylserine (PS), are almost completely localized in the inner leaflet of the plasma membrane.[4] Although the molecular level details are still ambiguous, it is clear that transmembrane asymmetry[5] is vital for a cell. PS transmembrane asymmetry was, for example, shown to regulate and maintain cell metabolism.[6,7] Transmembrane asymmetry can occur by means of active and passive pathways.[2,4] Active pathways use regulating proteins and peptides to induce asymmetry,[3,8,9] whereas passive pathways comprise several effects: a nonhomogeneous interleaflet charge distribution or hydration, asymmetry of specific interactions, and packing differences between leaflets. Although all of these effects have been studied, most attention has been given to transmembrane asymmetry as caused by a different available area in the inner and outer leaflet, which results in a different number of lipids in the inner and outer leaflet, and is related to local membrane stiffness and curvature.[10]

The investigation of passive asymmetry[11−22] is in general challenging as it ideally requires free floating, unperturbed, membranes. In addition, labeling, substrates, or invasive tools, which can induce changes to the bilayer composition, should ideally be avoided.[23] Sensitivity to molecular structure and the ability to distinguish between the inner and outer leaflet of a bilayer are further requirements. Vibrational sum frequency generation (SFG)[24−27] is a nonlinear spectroscopy that can be considered as a simultaneous IR and Raman measurement. SFG is forbidden in a centrosymmetric medium (under the dipole approximation[28]). It can therefore directly detect transmembrane asymmetry. Assuming identical orientational distributions with respect to the surface plane for lipids located on the inner and outer leaflets, SFG reports on the average number difference of lipids between the leaflets. These features were elegantly demonstrated by Conboy and co-workers who measured lipid redistribution across a supported planar bilayer that was initially made asymmetric.[12−14]

Here we investigate hydration, charge, and lipid transmembrane asymmetry in free floating lipid membranes. Lipid asymmetry and hydration in small unilamellar liposomes in solution (diameter <100 nm) are probed using nonlinear light scattering. By measuring vibrational sum frequency scattering (SFS) spectra in the C−H and P−O stretch region of the vibrational spectrum, we quantify the transmembrane asymmetry of the fatty acid tails and headgroups of the lipids. Vibrational SFS[29−31] is a combination of SFG and light

Received: November 10, 2015
Published: March 3, 2016

DOI: 10.1021/jacs.5b11776
J. Am. Chem. Soc. 2016, 138, 4053−4060

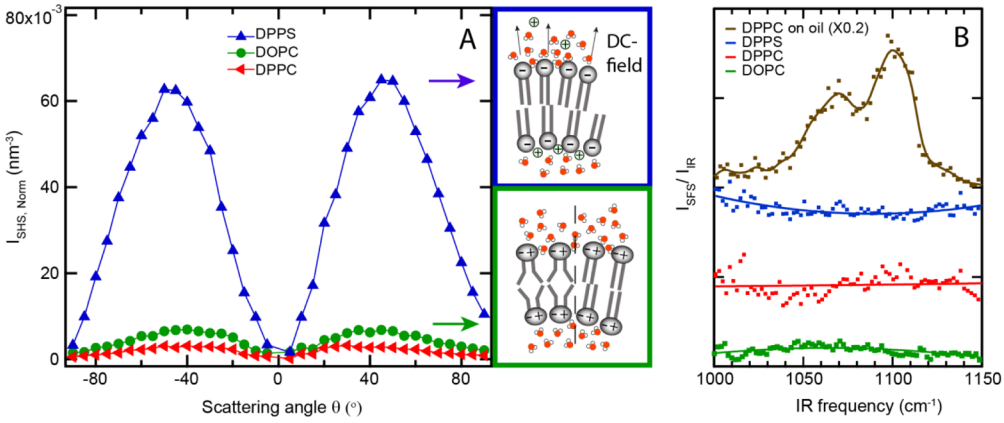

Figure 1. Liposome transmembrane asymmetry. A: SHS patterns measured with all beams polarized parallel to the scattering plane (PPP) of DPPS (blue), DOPC (green), and DPPC (red) liposomes in pure H_2O (0.8 mg/mL; extruded through a 100 nm pore). The scattering pattern originates from the overall transmembrane asymmetry in the orientational distribution of water molecules around the lipids (as illustrated in the cartoons). The data are scaled to correct for differences in size distribution and number density of the scatterers (as described in the SI, S2 and S3). B: SFS spectra of the same liposomes in D_2O in the P−O stretch region together with an SFS spectrum of hexadecane oil droplets covered with a DPPC monolayer (top trace). The spectra were collected with the IR (VIS, SF) beam polarized parallel (perpendicular) to the scattering plane (SSP). The SFS data are offset vertically for clarity.

scattering that allows for the probing of chemically specific molecular asymmetry along the interfacial normal in liposome membranes. Transmembrane hydration asymmetry is measured with nonresonant angle resolved[32] second harmonic scattering (SHS),[31,33,34] which probes transmembrane asymmetry in the orientational distribution of water molecules along the interfacial normal. The SHS signal relates to the surface potential[35−39] and to H-bond interactions involving water.[40] A change in the SHS intensity from liposomes is thus related to the difference in charge distribution between the leaflets. We find that charge and hydration asymmetry is present for liposomes made of 1,2-dioleoyl-*sn*-glycero-3-phosphocholine (DOPC), 1,2-dipalmitoyl-*sn*-glycero-3-phosphocholine (DPPC), 1,2- dipalmitoyl-*sn*-glycero-3-phosphoserine (DPPS), 1,2-dioleoyl-*sn*-glycero-3-phospho-L-serine (DOPS), and mixtures of either DOPC with DPPS or 1,2- dipalmitoyl-*sn*-glycero-3-phosphate (DPPA). Figure S1 displays a sketch of the chemical structure of each lipid. For the same single component liposomes, lipid transmembrane asymmetry is not detected, even though calculations using a constant area per lipid indicate a detectable difference in lipid number between the inner and outer leaflet. Binary mixtures may display transmembrane asymmetry, which can be detected in the phosphate stretch region as a shifted vibrational resonance. This PO_2^- group has a tilt angle with respect to the surface that is more upright, compared to the same groups in a lipid monolayer. A signature of the acyl chains is also observed, but only for one of the lipids. These observations only occur if phosphoserine is present in the binary bilayer mixture, and the acyl chains of the lipids are different in length. Based on these observations and the structure of the lipids, we postulate that lipid transmembrane asymmetry is likely induced by H-bonding interactions between amine and phosphate groups that depend on packing differences as induced by differences in fatty acid chain structure. Using this interpretation, we quantify the amount of asymmetry in the liposomes composed of a DOPC−DPPS mixture.

In what follows we first describe transmembrane hydration and lipid asymmetry for single component liposomes and then move on to binary mixtures. Finally, we aim to quantify the measured transmembrane asymmetry in terms of percentage number differences and differences in the orientational distributions of headgroups.

RESULTS AND DISCUSSION

Single Component Liposomes. Starting with lipid hydration, Figure 1A shows SHS patterns of single component liposomes made from DOPC, DPPC, and DPPS. The experimental procedure for the optical measurements can be found in section S1 of the Supporting Information. The data are scaled to correct for the difference in number density and size of the scatterers (see S2−3 for details). The SH signal is nonzero, which indicates that for these ∼100 nm diameter liposomes the hydration environment of the inner leaflet is different from the outer leaflet. Also, charged DPPS liposomes generate ∼21× more intensity per liposome than the zwitterionic, neutral liposomes. This difference can be explained by the interaction of the electrostatic field of the headgroup charge with the adjacent water molecules, which induces changes in the orientational distribution of the interfacial water molecules and hence increases the SHS intensity. This effect is absent for zwitterionic lipids. Thus, we observe a sizable asymmetry in the distribution of water molecules that is particularly sensitive to charge. Differently oriented hydrating water molecules in the inner and outer leaflets agree with the finding from X-ray, neutron, and dynamic light scattering that the electron density is asymmetrically distributed across the leaflets of anionic vesicles.[41] They also agree with the commonly employed assumption that the inner leaflet is considered charge-neutral.[36]

Does such transmembrane hydration asymmetry require transmembrane lipid asymmetry as well? According to calculations assuming a spherical geometry and constant lipid headgroup areas,[10] a number difference of 8% should be present between the inner and outer leaflet of these liposomes (see S6 for details). The difference in the number of lipids per leaflet can be estimated from SFS spectra, since SFS is exquisitely sensitive to transmembrane asymmetry. In particular, assuming a homogeneous distribution of lipid molecules, the SFS amplitude obtained from a sphere with a monolayer of

DOI: 10.1021/jacs.5b11776
J. Am. Chem. Soc. 2016, 138, 4053−4060

lipids on its surface is proportional to the averaged projection of the molecular tilt angle on the interfacial normal, multiplied by the number of lipids present in the probed area. For purposes of brevity we refer to this as the "projected surface density". For a liposome that has two oppositely oriented leaflets, the SFS amplitude reports on the transmembrane difference in projected surface density. Therefore, to quantify transmembrane lipid asymmetry, we measured with SFS the headgroup intensity in the P−O stretch region of liposomes as well as the headgroup intensity of a DPPC monolayer on 100 nm hexadecane droplets in water with a known molecular area of 0.48 nm^2 per DPPC molecule.[42] Knowing the area per lipid of the nanodroplet system, the size distribution of the droplets, and having a reasonable estimate of the average tilt angle of the P−N headgroup, we can compute the amplitude per lipid molecule, which can be used to derive a detection limit in terms of transmembrane lipid asymmetry. Assuming that the cross sections of the vibrational modes and average chain orientation are comparable, our previously derived detection limit[43] can be converted to a lower limit for the detectable transmembrane number difference of ∼2%.

Figure 1B shows SFS spectra of the same liposomes as in Figure 1A in the P−O stretch region: Within the signal-to-noise ratio of our instrument no apparent transmembrane lipid asymmetry is detected. For the C−H modes the same result was obtained (not shown). Thus, the lipid number difference for these single component liposomes is under our detection limit, meaning that the projected surface density difference is below 2%. Comparing this to the 8% in transmembrane lipid asymmetry,[10] that can be found from a computation considering constant headgroup areas per leaflet, it appears that a different lipid hydration does not require transmembrane lipid asymmetry in terms of a different number of lipids in the inner and outer leaflet. Instead, it may be influenced by specific lipid−lipid intermolecular interactions.[44] Such interactions would result in changes in the local (aqueous) environment of the lipids that can be probed in binary mixtures via the vibrational resonances of phospholipid headgroups.

The Phosphate Stretch Mode Is Sensitive to the Local Environment. The symmetric (s)-PO_2^- stretch mode has been shown to be very sensitive to changes in intermolecular and H-bonding interactions as well as the local aqueous environment. Counter ion induced shifts in the s-PO_2^- stretch mode have been reported.[45,46] Dehydration of a DPPC monolayer on a planar air/water interface results in a ∼10 cm^{-1} spectral shift of the s-PO_2^- mode to higher frequencies.[46] In order to verify that the s-PO_2^- stretch vibration is indeed a sensitive probe for changes in the local environment/lipid−lipid interactions, we have measured vibrational SFS spectra of hexadecane droplets covered with a dense monolayer of DPPC (analyzed in detail in ref 42) and of DPPE (1,2-dipalmitoyl-*sn*-glycero-3-phosphoethanolamine). It is worth noting that DPPE is different from DPPC in that it lacks the CH_3 groups around the N atom in the headgroup (Figure S1). For DPPE the amine and the phosphate group are expected to interact through intermolecular interactions,[10] which results in an increase of the gel phase transition temperature from 314 K for DPPC to 336 K for DPPE. The SFS spectra for DPPC and DPPE covered hexadecane droplets in water are shown in Figure 2A. The DPPC monolayer spectrum contains two peaks, one at ∼1070 cm^{-1}, assigned to the s-(C═O)−O−C stretch mode, and one at ∼1100 cm^{-1} assigned to the s-PO_2^- stretch mode of DPPC in a hydrated monolayer.[42,47−49] The DPPE monolayer

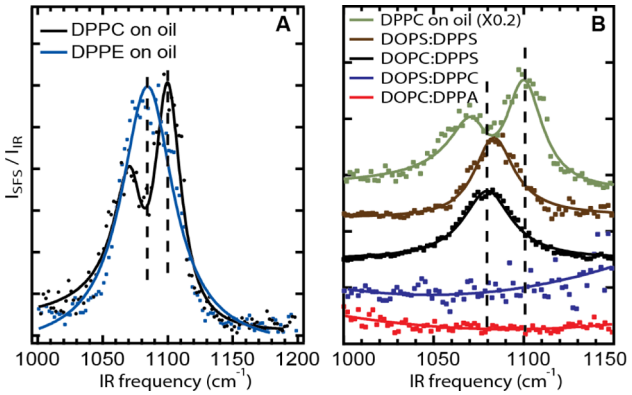

Figure 2. Transmembrane asymmetry. A: SFS spectra of DPPC (black) and DPPE (blue) monolayers on oil nanodroplets at maximum lipid coverage measured using the SSP polarization combination. The dashed lines show the positions of the PO_2^- symmetric stretch modes in DPPC and DPPE. B: SFS (SSP) spectra taken in the P−O stretch region of ∼100 nm diameter liposomes in pure D_2O composed of 1:1 mixtures of DOPS−DPPS (brown), DOPC−DPPS (black), DOPS−DPPC (blue), and DOPC−DPPA (red) and the P−O spectrum of the liquid condensed like DPPC monolayer (with known headgroup area) on oil droplets (green). The SFS data are offset vertically for clarity.

spectrum is different: it shows a single peak at ∼1080 cm^{-1}. Based on the demonstrated sensitivity of the s-PO_2^- stretch mode on the local environment at the air/water interface, this peak likely originates from a population of H-bonded PE groups resulting in red-shifted[50] s-PO_2^- stretch modes. In addition, since the s-PO_2^- mode consists of an isolated vibrational resonance, it can easily be used to obtain the orientational distribution of the headgroups.

In what follows we use this mode as a probe to study transmembrane lipid asymmetry in liposomes composed of two different lipids. As a starting point, studies of giant unilamellar vesicles composed of PS lipids and a lipid of different acyl chain lengths[51,52] can be used. These mixtures display phase separation behavior as a function of acyl chain conformation and thus may exhibit a certain amount of transmembrane asymmetry.

Liposomes from Binary Mixtures. Figure 2B shows SFS spectra of liposomes in the P−O stretch region composed of a 1:1 mixture of DOPC−DPPS, DOPS−DPPC, DOPS−DPPS, and DOPC−DPPA. As a comparison, the P−O signal from the DPPC monolayer is also shown (green curve). It can be seen that the DOPC−DPPS liposomes generate a nonzero SF spectrum. Compared to the spectrum of the PC headgroups in a DPPC monolayer, there is a single peak at ∼1080 cm^{-1}. Based on the comparison between DPPC and DPPE monolayers in Figure 2A, the 1080 cm^{-1} mode is likely assigned to a population of H-bonded s-PO_2^- stretch modes. Liposomes composed of a 1:1 DOPS−DPPC mixture possess the same headgroup chemistry, but they will likely have a different packing. It can be seen from Figure 2B that these liposomes do not generate any detectable SFS intensity. Thus, in these mixtures, all of the lipid headgroups are distributed symmetrically across both leaflets (within the detection limit). The same is also true for DOPS−DOPC and DPPS−DPPC mixtures (see Figure S2 in the Supporting Information). Removing the amine group but keeping the negative charge as in a DOPC−DPPA mixture also results in an absence of transmembrane asymmetry.

DOI: 10.1021/jacs.5b11776
J. Am. Chem. Soc. 2016, 138, 4053−4060

Since the phosphate groups in the PA and PS headgroups are likely equally well-hydrated, it appears, based on the observed differences in intensity, that a charged lipid with a free amine group is crucial for the observed transmembrane asymmetry. This apparent PS specificity is further investigated by measuring single lipid DOPS liposomes and DOPS−DPPS liposomes. The former displays a comparable hydration asymmetry as DPPS, with no apparent transmembrane asymmetry (data not shown). A 1:1 DOPS−DPPS mixture, however, which possesses the same headgroup chemistry and the same difference in fatty acid tail chemistry as the DOPC−DPPS liposomes does display transmembrane asymmetry (Figure 2B). For this binary lipid mixture, we observe the s-PO_2^- stretch mode at 1085 cm^{-1}, thus with a comparable frequency and intensity as for DOPC−DPPS liposomes. The measured PO_2^- modes represent the population of asymmetrically distributed phosphate groups between the leaflets.

In what follows we formulate a hypothesis to rationalize where this PO_2^- signal originates from and how intermolecular interactions are created.

Lipid−Lipid Interactions Drive Transmembrane Asymmetry? As Figure 2B shows, in order to establish transmembrane asymmetry in the studied systems, charged PS headgroups are crucial ingredients. PS headgroups possess oppositely charged phosphate, carboxylate and amine groups, which can each participate in H-bonding interactions with a neighboring lipid and with water.[15,44,53] NH_4^+ ions as well as NH_3^+ groups are known to interact with PO_4^- groups of neighboring molecules[53−55] (in the fashion illustrated in Figure 3A). However, as Figure 1 shows, no transmembrane lipid asymmetry is observed for pure DPPS liposomes, indicating that an additional criterion needs to be satisfied. Namely, a difference in the fatty acid chain length and associated packing appears to be necessary, as is also corroborated by the aforementioned studies on giant unilamellar vesicles.[51,52] We also confirmed that the s-PO_2^- stretch mode is sensitive to the local environment. Observing a similar red shift in the phosphate stretch mode as in the DPPE monolayer that exhibit headgroup−headgroup H-bonding interactions, it seems likely that intermolecular interactions are also crucial here.

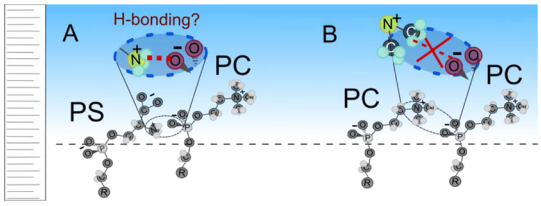

Figure 3. H-bonding interactions between lipids. The H-bonding interaction between phospholipid headgroups is determined by the lipid structure and by the headgroup- and fatty acid tail chemistry. A: For a PS−PC pair the $H_2N-H^{\cdots}O-PO$ H-bond may be present depending on the distance between lipid headgroups (which can be changed by selecting proper combination of fatty acid tails). B: In contrast, for a PC−PC pair the headgroup chemistry is different, and there is no possible intermolecular H-bonding.

Figure 3A and B illustrate one possibility to explain the observed data: PS−PC headgroups may interact through $H_2N-H^{\cdots}O-PO$ H-bonding, which would shift the vibrational frequency of the interacting phosphate groups (on the PC lipids) to a lower frequency. In doing so, they become SFS active. This interaction can, however, only occur if the probability of intermolecular interactions is increased (compared to the pure DPPS or DOPS liposomes). By changing the lipid tails from DO (18 C atoms, one unsaturated bond) to the ∼1 Å shorter DP tails[56] (16 C atoms, saturated) the distance between the H_2N-H and the O−PO groups is reduced, facilitating more favorable intermolecular interactions[15] in a mixture of DOPC with DPPS or DOPS with DPPS. Although this explanation agrees with the presented data, it will have to be investigated in more detail, e.g., by employing molecular dynamics simulations.

Using this explanation and the C−H mode signal as a probe for lipid transmembrane asymmetry and the phosphate stretch mode signal as a probe for (DOPC) lipids that are interacting with DPPS lipids, we quantify both types of transmembrane asymmetry in the DOPC−DPPS liposomes.

Quantifying Transmembrane Asymmetry. To determine the percentage of lipids that are asymmetrically distributed across the membrane, we use selective deuteration and measure SFS spectra in the C−H stretch mode region, targeting the lipid fatty acid tails. Since C−D modes vibrate at different frequencies, the amount of lipid transmembrane asymmetry can be determined (as the C−H modes are insensitive to changes in the local environment).

Figure 4A shows SFS spectra of liposomes in the C−H stretch region composed of a 1:1 mixture of d_{66}-DOPC−DPPS and DOPC−d_{62}-DPPS. The C−H mode signal from the DPPC monolayer on oil droplets is shown in the top trace for comparison. The C−H mode region is comprised of the following peaks:[29,49,57,58] the s-CH_2 stretch mode (∼2852 cm^{-1}, d^+), the s-CH_3 stretch mode (∼2876 cm^{-1}, r^+), the antisymmetric (as) CH_3 stretch mode (∼2965 cm^{-1}, r^-), the s-CH_2−Fermi resonance (∼2919 cm^{-1}, d^+_{FR}), the s-CH_3−Fermi resonance (∼2935 cm^{-1}, r^+_{FR}), and the as-CH_2 stretch mode (∼2905 cm^{-1}, d^-). It can be seen that the s-CH_3 stretch mode is dominant for the monolayer on droplets, which means that the alkyl chains are nearly all-trans in their conformation.[42] The liposomes with PS and PC mixtures display only a detectable SF response in the case of the d_{66}-DOPC−DPPS mixture, which indicates that only the DPPS molecules are asymmetrically distributed across the bilayer, and not the DOPC molecules (assuming that the deuteration procedure does not change any lipid properties, which is generally expected to be the case[59]). The SF spectrum of the DPPS molecules shows a prominent peak at 2870 cm^{-1}, which corresponds to the s-CH_3 stretch mode, while very little intensity is observed at 2850 cm^{-1}, indicating an all-trans conformation of the tails (identical to that of DPPC). We thus assume that the DP acyl tail conformations in both systems are equal. Comparing the obtained SFS intensity (α) of the s-CH_3 stretch mode for the d_{66}-DOPC−DPPS liposomes to that of the DPPC monolayer, we find a transmembrane asymmetry in terms of the surface number density ratio ($n_{lip,DPPS}/n_d$) of:

$$\sqrt{\frac{\alpha_{lip}}{\alpha_d}}(C-H) = \frac{n_{lip,DPPS}}{n_d} \quad (1)$$

where α is scaled in order to be independent of the size of the droplet/liposome (see eqs 11−13 in the SI and sections S2, S3, and S7 for a derivation of all parameters). From eq 1, the transmembrane asymmetry is then determined for DPPS to be $n_{lip,DPPS}/n_d = 0.16$ (i.e., ∼58% of the DPPS molecules is located on the outer leaflet and ∼42% of the DPPS molecules is located

DOI: 10.1021/jacs.5b11776
J. Am. Chem. Soc. 2016, 138, 4053−4060

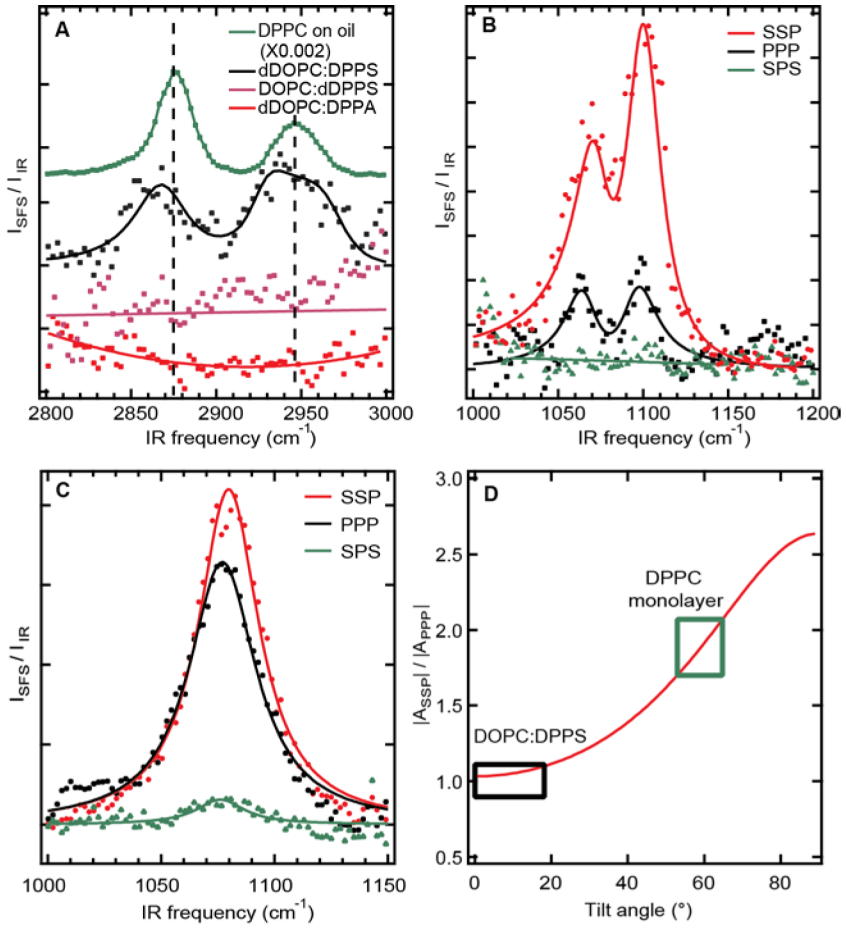

Figure 4. Quantifying transmembrane asymmetry. A: SFS (SSP) spectra taken in the C−H stretch region of ∼100 nm diameter liposomes in pure water composed of 1:1 mixtures of d_{66}-DOPC−DPPS (black), DOPC−d_{62}-DPPS (purple), and d_{66}-DOPC:DPPA (red) and the spectrum of the DPPC monolayer on oil droplets (green). The solid lines represent fits to the data. The SFS data are offset vertically for clarity. B: SFS spectra of a DPPC monolayer on oil droplets, recorded in SSP (red), PPP (black), and SPS (green) polarization combinations. C: SFS spectra of DOPC−DPPS liposomes in SSP (red), PPP (black), and SPS (green) polarization combinations. D: Dependence of the amplitude ratio of the SSP and PPP polarization combinations of the s-PO_2^- stretch mode on the tilt angle (details of the computation can be found in section S5 of the SI). The boxes indicate the measured ratios obtained from the spectra in panels B and C.

on the inner leaflet, assuming similar sizes for DPPS and DPPC).

The orientational distribution $<\cos\phi_d>$ ($<\cos\phi_{lip}>$) of the asymmetrically distributed phosphate headgroups on the DPPC covered droplets (DOPC−DPPS liposomes) can be estimated from polarization-dependent SFS spectra. The data are shown in Figure 4B and C. The angle ϕ represents the tilt angle of the symmetry axis of the s-PO_2^- mode with the surface normal of the liposome or droplet. To determine $<\cos\phi_d>$, the orientational analysis for polarization resolved SFS[42,60] is extended to include a relationship between the second-order susceptibility and hyperpolarizability elements that uses a tilt (ϕ) and a twist (ψ) angle for the phosphate group. We follow here the procedure as introduced by the Allen lab.[46] The computed amplitude polarization ratio for the s-PO_2^- stretch mode for the case that $\psi = 0$[46] is displayed as a function of tilt angle in Figure 4D. The experimentally measured scattering amplitude ratios obtained from Figures 4B and C are indicated as rectangular areas in Figure 4D and show that the phosphate groups of the DPPC molecules situated on oil droplets have an average tilt angle of $\phi = 60 \pm 10°$ with respect to the droplet surface normal. Note that this is an advancement of the analysis in ref 42. The calculated value is in good agreement with the tilt angle found for DPPC molecules at the air/water interface.[46] For the liposomes we find a tilt angle of $\phi = 10 \pm 10°$. More details about the analysis can be found in the SI, in S4 and S5. Note that we have assumed a narrow Gaussian distribution for the tilt angle, as well as a uniform distribution of lipids. The latter is expected[61] since we have not detected any SFS signal in the polarization combinations PSP, PPS, and SPP. Using a Gaussian distribution may not be completely justifiable since the number of participating lipids (several thousand) are not sufficient to make a statistical distribution.

To estimate the percentage of DOPC molecules that interact with DPPS, we compare the s-PO_2^- mode amplitude of the DOPC:DPPS mixtures and the DPPC monolayer. We use the following expression:

$$\sqrt{\frac{\alpha_{lip}}{\alpha_d}}(P-O) = \frac{n_{lip,DOPC}<\cos(\phi_{lip})>}{n_d<\cos(\phi_d)>} \quad (2)$$

The ratio $(\alpha_{lip}/\alpha_d)^{1/2}(P-O)$ represents the amplitude ratio of the s-PO_2^- mode of the lipids in the liposomes and the droplet monolayers (corrected for the difference in droplet/liposome number density and size distribution). This number reports only on the head groups that exhibit intermolecular

DOI: 10.1021/jacs.5b11776
J. Am. Chem. Soc. 2016, 138, 4053−4060

interactions, and thus likely on DOPC molecules. The ratio $n_{lip,DPPS}/n_d$ represents the number density ratio of the interacting DOPC lipids in the liposomes compared to the DPPC number density on the droplets. The orientational distribution is represented by $<\cos\phi>$, as discussed in the previous paragraph. From Figure 4A we have $(\alpha_{lip}/\alpha_d)^{1/2}(P-O) = 0.9 \pm 0.3$. The factor $<\cos\phi_{lip}>/<\cos\phi_d> = 2$. From eq 2 we then have $n_{lip,DPPS}/n_d = 0.45$. This means effectively that all the DOPC molecules in the outer leaflet are interacting with DPPS molecules. Note that in this analysis we implicitly assumed that the inner leaflet is charge neutral.[36] Since this means that the Na^+ counterions are in close proximity to the PS headgroups (but likely not ion paired so that no frequency shifts are detectable[62]), it will result in a much lower probability for intermolecular H-bonding in the inner leaflet between PS and PC headgroups.

Thus, from the analysis of the spectra in Figures 2 and 4 (and relying on the interpretation in Figure 3), we find that there is a lipid number difference of ∼16% of DPPS between the inner and outer leaflets. There is no detectable difference in the number of DOPC lipids between the outer and inner leaflets. The shifted s-PO_2^- SFS response from the liposomes indicates that some of the DOPC molecules interact with DPPS through intermolecular H-bonding, which significantly alters the orientation of the headgroups toward a more parallel orientation with respect to the surface plane. Assuming charge neutrality in the interior, and a consequential lack of intermolecular H-bonds, we find that nearly all of the DOPC in the outer leaflet interacts with DPPS.

CONCLUSIONS

We find that charge and hydration transmembrane asymmetry is present in liposomes in aqueous solution, while for the same single component liposomes lipid transmembrane asymmetry is not detectable. Asymmetry in the number of lipids per leaflet can be induced by H-bond interactions between PS and PC/PS headgroups that depend on and can be influenced by varying the lipid structure. DOPC−DPPS liposomes exhibit a 16% DPPS asymmetry but no detectable DOPC asymmetry. The P−O vibrational stretch mode intensity becomes clearly observable, indicating transmembrane asymmetry. This is related to a different orientational distribution of PC phosphate groups that participate in H-bond interactions with the PS amine groups. In particular we find that the average orientational angle with respect to the surface normal of the phosphate group becomes close to 10°, which is substantially different from the 60° that is found in a saturated monolayer. This indicates that in the liposomes the interacting headgroups of the DOPC are aligned along the interface (and thus occupy a maximum volume).

The presence of lipid transmembrane asymmetry and probable underlying mechanism offer insights into the complexity of lipid membrane chemistry. If specific/chemical interactions lead to association of molecules in a 100 nm liposome, then it is likely that similar mechanisms can play a role in the formation and stabilization of lipid domains. Lipid rafts are considered to be dynamic structures >40 nm in size that form and dissolve on millisecond time scales.[63] As such our work provides insights into how these domains might form. Future work that is geared at further understanding the link between the transmembrane asymmetry studied here and lipid raft structure might involve nonlinear scattering experiments performed in all polarization combinations, which is sensitive to structural heterogeneities.[61] These measurements should be performed on liposomes with a diameter of ∼10 μm, to enable the formation of multiple domains and to obtain good signal-to-noise ratios.

Given the importance of membrane properties and liposomes in basic biophysical research and biotechnology, our combination of SF and SH scattering techniques demonstrates a high potential to elucidate transmembrane asymmetry in lipid membranes. Particularly, these methods can be used to investigate lipid asymmetry induced by drug−membrane or biomacromolecule−membrane interactions along with domain formation in lipid mixtures.

MATERIALS AND METHODS

Chemicals. Prior to use all glassware was cleaned with a 1:3 H_2O_2−H_2SO_4 solution, after which it was thoroughly rinsed with ultrapure water (H_2O, Milli-Q UF Plus, Millipore, Inc., electrical resistance of 18.2 MΩ cm). d_{34}-hexadecane ($C_{16}D_{34}$, 98% d, Cambridge Isotope), sulfuric acid (95−97%, ISO, Merck), H_2O_2 (30%, Reactolab SA), and chloroform (Emsure, ACS, ISO, Merck) was used as received. Lipids 1,2-dioleoyl-*sn*-glycero-3-phosphocholine (DOPC), 1,2-dipalmitoyl-*sn*-glycero-3-phosphocholine (DPPC), 1,2-dioleoyl-*sn*-glycero-3-phospho-L-serine (sodium salt) (DOPS), 1,2-dipalmitoyl-*sn*-glycero-3-phospho-L-serine (sodium salt) (DPPS), 1,2-dipalmitoyl-*sn*-glycero-3-phosphate (sodium salt) (DPPA), 1,2-dipalmitoyl-*sn*-glycero-3-phosphoethanolamine (DPPE), d_{62}-1,2-dipalmitoyl-*sn*-glycero-3-phospho-L-serine (sodium salt) (d_{62}-DPPS), and d_{66}-1,2-dioleoyl-*sn*-glycero-3-phosphocholine (d_{66}-DOPC), were purchased in powder form (>99%) from Avanti Polar Lipids (Alabama, USA) and stored at −20 °C until further use. All samples for SFS measurements were prepared using D_2O (99.8% Armar, >2 MΩ cm). The chemical structures of the used lipids are presented in Figure S1.

Droplet Preparation. Nanodroplets with a phospholipid monolayer were prepared according to the procedure described in ref 42. We used 1 mM DPPC or DPPE on 2 vol % *d*-hexadecane which gives saturated monolayer of lipid on oil droplets. The droplet size distribution was measured with dynamic light scattering (DLS, Zetasizer Nano ZS, Malvern). The droplets had a mean diameter of ∼200 nm with a polydispersity index (PDI) of ∼0.2.

Liposomes. Small unilamellar vesicles were prepared by extrusion according to refs 64 and 65. Lipid stock solutions were created by dissolving the lipid powder in chloroform in a 4 mL glass vial with a PTFE screw cap. Stocks were stored at −20 °C, but not for more than 6 months. First, multilamellar vesicles were created by pipetting the desired amounts of lipid stock solutions into a round-bottom glass tube using a glass syringe (Hamilton). When a mixture of different lipids was used, the desired amounts of the various lipid solutions were mixed together. While rotating the glass tube, a nitrogen gas stream was directed into the tube to evaporate the chloroform. The resulting lipid film was further dried in vacuum (<100 mbar, created by an oil-free diaphragm pump) at room temperature for at least 2 h. Finally, the lipid film was resuspended in D_2O or H_2O and vortexed. To create unilamellar vesicles, the resulting multilamellar vesicle solutions were extruded with a Miniextruder (AvantiPolarLipids, Al) using a polycarbonate membrane with a pore diameter of 100 nm at room temperature (or above their respective lipid transition temperature). Unilamellar vesicles were stored in closed containers up to 2 weeks at 4 °C. The size and zeta-potential distribution of the liposomes were measured with DLS and laser Doppler electrophoresis at 25 °C (Malvern ZS nanosizer). To determine the size distribution of the vesicles, three subsequent measurements, each 11 runs, were averaged. To determine the zeta potential of the vesicles three subsequent measurements, each 75 runs at automated voltage, were averaged. The liposomes were found to have a mean diameter in the range of 70−100 nm with a polydispersity index (PDI) of less than 0.1. The final lipid concentration was determined using a calorimetric phosphorus assay; for further details, see ref 66. The concentration of the lipids in the sample was 0.8 mg lipids/mL weight ratio for DLS, zeta potential

DOI: 10.1021/jacs.5b11776
J. Am. Chem. Soc. 2016, 138, 4053−4060

measurements, and SHS experiments. For sum frequency scattering the sample concentration was ∼5 mg/mL. The mean values of DLS and zeta potential measurements are summarized in Table S1 including the standard deviations of the mean from three consecutive measurements. The standard deviation of the distribution in a single measurement was 10% and 20% for size- and zeta potential measurements, respectively.

■ ASSOCIATED CONTENT

Supporting Information

The Supporting Information is available free of charge on the ACS Publications website at DOI: 10.1021/jacs.5b11776.

Details about the lipids and the measurement methods (S1), the normalization and correction procedures that were used to correct for the difference in size distribution (S2), the procedure to calculate an effective radius (S3), the spectral fitting procedure for SFS data (S4), details for the calculation of the orientational distribution of phosphate groups (S5), details for the calculations of the degree of asymmetry based on geometrical arguments and as derived from SFS data (S6/S7), and additional SFS experiments (S8) (PDF)

■ AUTHOR INFORMATION

Corresponding Author

*sylvie.roke@epfl.ch

Author Contributions

‡N.S. and C.L. contributed equally.

Notes

The authors declare no competing financial interest.

■ ACKNOWLEDGMENTS

This work is supported by the Julia Jacobi Foundation and the European Research Council (grant numbers 240556 and 616305). We thank Yixing Chen for the measurements in Figure 2A.

■ REFERENCES

(1) Binder, W. H.; Barragan, V.; Menger, F. M. *Angew. Chem., Int. Ed.* **2003**, *42*, 5802.
(2) van Meer, G.; Voelker, D. R.; Feigenson, G. W. *Nat. Rev. Mol. Cell Biol.* **2008**, *9*, 112.
(3) Leventis, P. A.; Grinstein, S. *Annu. Rev. Biophys.* **2010**, *39*, 407.
(4) van Meer, G.; de Kroon, A. *J. Cell Sci.* **2011**, *124*, 5.
(5) Yeagle, P. L.; Hutton, W. C.; Martin, R. B. *J. Biol. Chem.* **1976**, *251*, 2110.
(6) Fadok, V. A.; Henson, P. M. *Curr. Biol.* **1998**, *8*, R693.
(7) Cong, X.; Poyton, M. F.; Baxter, A. J.; Pullanchery, S.; Cremer, P. S. *J. Am. Chem. Soc.* **2015**, *137*, 7785.
(8) Frechin, M.; Enkler, L.; Tetaud, E.; Laporte, D.; Senger, B.; Blancard, C.; Hammann, P.; Bader, G.; Clauder-Munster, S.; Steinmetz, L. M.; Martin, R. P.; di Rago, J. P.; Becker, H. D. *Mol. Cell* **2014**, *56*, 763.
(9) Frechin, M.; Stoeger, T.; Daetwyler, S.; Gehin, C.; Battich, N.; Damm, E.-M.; Stergiou, L.; Riezman, H.; Pelkmans, L. *Nature* **2015**, *523*, 88.
(10) Israelachvili, J. N. *Intermolecular and surface forces*; Academic Press: New York, 1991.
(11) Siu, S. W. I.; Vacha, R.; Jungwirth, P.; Bockmann, R. A. *J. Chem. Phys.* **2008**, *128*, 125103.
(12) Brown, K. L.; Conboy, J. C. *J. Am. Chem. Soc.* **2011**, *133*, 8794.
(13) Anglin, T. C.; Conboy, J. C. *Biophys. J.* **2008**, *95*, 186.
(14) Liu, J.; Conboy, J. C. *J. Am. Chem. Soc.* **2004**, *126*, 8376.
(15) Berkowitz, M.; Pandit, S. *Biophys. J.* **2003**, *84*, 46a.
(16) Mondal, S.; Mukhopadhyay, C. *Langmuir* **2008**, *24*, 10298.
(17) Vacha, R.; Siu, S. W. I.; Petrov, M.; Bockmann, R. A.; Barucha-Kraszewska, J.; Jurkiewicz, P.; Hof, M.; Berkowitz, M. L.; Jungwirth, P. *J. Phys. Chem. A* **2009**, *113*, 7235.
(18) Cascales, J. J. L.; Otero, T. F.; Smith, B. D.; Gonzalez, C.; Marquez, M. *J. Phys. Chem. B* **2006**, *110*, 2358.
(19) Kiessling, V.; Wan, C.; Tamm, L. K. *Biochim. Biophys. Acta, Biomembr.* **2009**, *1788*, 64.
(20) Nakano, M.; Fukuda, M.; Kudo, T.; Endo, H.; Handa, T. *Phys. Rev. Lett.* **2007**, *98*, 238101.
(21) Veatch, S. L.; Polozov, I. V.; Gawrisch, K.; Keller, S. L. *Biophys. J.* **2004**, *86*, 2910.
(22) Serebryany, E.; Zhu, G. A.; Yan, E. C. Y. *Biochim. Biophys. Acta, Biomembr.* **2012**, *1818*, 225.
(23) Richter, R. P.; Berat, R.; Brisson, A. *Langmuir* **2006**, *22*, 3497.
(24) Hunt, J. H.; Guyot-Sionnest, P.; Shen, Y. R. *Chem. Phys. Lett.* **1987**, *133*, 189.
(25) Harris, A. L.; Chidsey, C. E. D.; Levinos, N. J.; Loiacono, D. N. *Chem. Phys. Lett.* **1987**, *141*, 350.
(26) Yan, E. C. Y.; Wang, Z.; Fu, L. *J. Phys. Chem. B* **2015**, *119*, 2769.
(27) Johnson, C. M.; Baldelli, S. *Chem. Rev.* **2014**, *114*, 8416.
(28) Boyd, R. W. *Nonlinear Optics*, 3rd ed.; Academic Press: Burlington, 2008.
(29) Roke, S.; Roeterdink, W. G.; Wijnhoven, J. E. G. J.; Petukhov, A. V.; Kleyn, A. W.; Bonn, M. *Phys. Rev. Lett.* **2003**, *91*, 258302.
(30) Strader, M. L.; de Aguiar, H. B.; de Beer, A. G. F.; Roke, S. *Soft Matter* **2011**, *7*, 4959.
(31) Roke, S.; Gonella, G. *Annu. Rev. Phys. Chem.* **2012**, *63*, 353.
(32) Schürer, B.; Wunderlich, S.; Sauerbeck, C.; Peschel, U.; Peukert, W. *Phys. Rev. B: Condens. Matter Mater. Phys.* **2010**, *82*, 241404.
(33) Wang, H.; Yan, E. C. Y.; Borguet, E.; Eisenthal, K. B. *Chem. Phys. Lett.* **1996**, *259*, 15.
(34) Eisenthal, K. B. *Chem. Rev.* **2006**, *106*, 1462.
(35) Liu, J.; Subir, M.; Nguyen, K.; Eisenthal, K. B. *J. Phys. Chem. B* **2008**, *112*, 15263.
(36) Liu, Y.; Yan, C. Y.; Zhao, X. L.; Eisenthal, K. B. *Langmuir* **2001**, *17*, 2063.
(37) Rao, Y.; Kwok, S. J. J.; Lombardi, J.; Turro, N. J.; Eisenthal, K. B. *Proc. Natl. Acad. Sci. U. S. A.* **2014**, *111*, 12684.
(38) Yan, E. C. Y.; Liu, Y.; Eisenthal, K. B. *J. Phys. Chem. B* **2001**, *105*, 8531.
(39) de Beer, A. G. F.; Campen, R. K.; Roke, S. *Phys. Rev. B: Condens. Matter Mater. Phys.* **2010**, *82*, 235431.
(40) Scheu, R.; Rankin, B. M.; Chen, Y. X.; Jena, K. C.; Ben-Amotz, D.; Roke, S. *Angew. Chem., Int. Ed.* **2014**, *53*, 9560.
(41) Anghel, V. N. P.; Kucerka, N.; Pencer, J.; Katsaras, J. *J. Appl. Crystallogr.* **2007**, *40*, 513.
(42) Chen, Y.; Jena, K. C.; Lütgebaucks, C.; Okur, H. I.; Roke, S. *Nano Lett.* **2015**, *15*, 5558.
(43) Jena, K. C.; Scheu, R.; Roke, S. *Angew. Chem., Int. Ed.* **2012**, *51*, 12938.
(44) Pandit, S. A.; Bostick, D.; Berkowitz, M. L. *Biophys. J.* **2003**, *85*, 3120.
(45) Casal, H. L.; Mantsch, H. H.; Paltauf, F.; Hauser, H. *Biochim. Biophys. Acta, Lipids Lipid Metab.* **1987**, *919*, 275.
(46) Casillas-Ituarte, N.; Chen, X.; Castada, H.; Allen, H. C. *J. Phys. Chem. B* **2010**, *114*, 9485.
(47) Chen, X.; Allen, H. C. *J. Phys. Chem. A* **2009**, *113*, 12655.
(48) Chen, X.; Hua, W.; Huang, Z.; Allen, H. C. *J. Am. Chem. Soc.* **2010**, *132*, 11336.
(49) Liljeblad, J. D. F.; Bulone, V.; Tyrode, E.; Rutland, M. W.; Johnson, C. M. *Biophys. J.* **2010**, *98*, L50.
(50) Although the mode at 1080 cm^{-1} could in principle be assigned to both modes, the s-(C═O)−O−C stretch mode is not involved in any lipid specific interaction, which means it is an unlikely candidate for the assignment.
(51) Shimokawa, N.; Hishida, M.; Seto, H.; Yoshikawa, K. *Chem. Phys. Lett.* **2010**, *496*, 59.
(52) Bandekar, A.; Sofou, S. *Langmuir* **2012**, *28*, 4113.
(53) Pandit, S. A.; Berkowitz, M. L. *Biophys. J.* **2002**, *82*, 1818.

DOI: 10.1021/jacs.5b11776
J. Am. Chem. Soc. 2016, 138, 4053−4060

(54) Petrache, H. I.; Tristram-Nagle, S.; Gawrisch, K.; Harries, D.; Parsegian, V. A.; Nagle, J. F. *Biophys. J.* **2004**, *86*, 1574.
(55) Mukhopadhyay, P.; Monticelli, L.; Tieleman, D. P. *Biophys. J.* **2004**, *86*, 1601.
(56) Nagle, J. F.; Tristram-Nagle, S. *Biochim. Biophys. Acta, Rev. Biomembr.* **2000**, *1469*, 159.
(57) Walker, R. A.; Conboy, J. C.; Richmond, G. L. *Langmuir* **1997**, *13*, 3070.
(58) Liu, J.; Conboy, J. C. *Biophys. J.* **2005**, *89*, 2522.
(59) Tokutake, N.; Jing, B.; Cao, H.; Regen, S. L. *J. Am. Chem. Soc.* **2003**, *125*, 15764.
(60) de Beer, A. G. F.; Roke, S. *J. Chem. Phys.* **2010**, *132*, 234702.
(61) de Beer, A. G. F.; Roke, S.; Dadap, J. I. *J. Opt. Soc. Am. B* **2011**, *28*, 1374.
(62) van der Vegt, N. F. A.; Roke, S.; Zheng, J.; Lund, M.; Bakker, H. J. *Chem. Rev.* **2016**, submitted.
(63) Honigmann, A.; Mueller, V.; Hell, S. W.; Eggeling, C. *Faraday Discuss.* **2013**, *161*, 77.
(64) Hope, M. J.; Bally, M. B.; Webb, G.; Cullis, P. R. *Biochim. Biophys. Acta, Biomembr.* **1985**, *812*, 55.
(65) Macdonald, R. C.; Macdonald, R. I.; Menco, B. P. M.; Takeshita, K.; Subbarao, N. K.; Hu, L. R. *Biochim. Biophys. Acta, Biomembr.* **1991**, *1061*, 297.
(66) Chen, P. S.; Toribara, T. Y.; Warner, H. *Anal. Chem.* **1956**, *28*, 1756.

DOI: 10.1021/jacs.5b11776
J. Am. Chem. Soc. 2016, 138, 4053−4060